Indian Journal of Pure & Applied Physics
Vol. 64, August 2026, pp. 936-942
DOI: 10.56042/ijpap.v64i8.31544

Temperature-Dependent Conductivity of Polypyrrole and Polypyrrole/ZnO Nanocomposite

Dimple Balan[a*], Minakshi[b], Ravinder Kumar[a], Chetan Sharma[c] & Devendra Mohan[d]

[a]Department of Physics, Guru Jambheshwar University of Science & Technology, Hisar 125 001, India

[b]Department of Physics, CMG GCW BhodiaKhera, Fatehabad 125 050, India

[c]Department of Physics, Dayanand College, Hisar 125 001, India

[d]Department of Applied Science, Panipat Institute of Engineering and Technology, Samalkha, Haryana 132 102, India

Received: 14th May 2026; accepted: 2nd July 2026

Polypyrrole (Ppy) and polypyrrole/zinc oxide (Ppy/ZnO) nanocomposites were prepared using a chemical oxidative polymerization method. Methyl orange was used as a soft-template surfactant to help spread the particles evenly and control their shape during the polymerization. These nanocomposites are studied for their temperature-dependent electrical conductivity. Ppy was mixed during synthesis with 5 wt % zinc oxide to improve its electrical and chemical characteristics. Field Emission Scanning Electron Microscopy (FESEM) analysis indicates that the nanocomposites have a cylindrical surface structure. In addition, the structural nature of the Ppy/ZnO nanocomposites is amorphous in nature, as indicated by the X-ray diffraction patterns. The Ppy/ZnO nanocomposites are ideal materials for various applications because they have high electrical conductivity that varies with temperature.

Keywords: Conductivity, Polypyrrole, Conducting polymer, Nanocomposites, Zinc oxide

1 Introduction

Nanocomposites and/or heterostructure formation is the subject of new techniques for enhancing the physico-chemical properties of existing available nanomaterials[1-6]. This may lead to the formation of new and advanced materials of improved properties by controlling the shape, structure, and combination of two different types of nanostructures, i.e., organic and inorganic nanostructures[7-9]. The change in electric properties caused by interface effects and quantum effects produced by nano dimensions is significant in showing the final quality. The set of properties that is desired may be tailored and/or developed by using a combination of both of these effects. Moreover, these new materials, also called nanocomposites or heterostructures, have been synthesized with regard to their possible application in gas sensors, vacuum micro/nano electronics, photo catalysis, hydrogen production, Supercapacitor, and optoelectronics[10–14]. The advantages of field emission (FE) based emitters over conventional thermionic electron sources in vacuum microelectronic devices are unprecedented at this time[15].Conducting polymers featuring a π-electron–conjugated backbone such as polypyrrole (Ppy), polyaniline, and polythiophene have attracted significant interest for gas-sensing applications[16-18]. Their detection capability is primarily governed by the doping and de-doping processes (oxidation and reduction), enabling selective interaction with particular gas molecules[19]. Among them, Ppy has shown measurable and distinct responses to a wide range of vapours, including acids, bases, alcohols, and alkanes, due to its unique interaction mechanisms[20–24]. Key advantages of Ppy include its simple synthesis process, high environmental stability, and electrochromic properties[25, 26]. It can be prepared by several methods, such as the chemical or catalytic oxidation of the electrochemical polymerization[27] or pyrrole monomer[28]. Thin films of CP in the micro or nanometer range have higher gas sensitivity than bulk films[29]. The use of nanoparticles in Ppy films changes their electrical conductivity. For example, in Ppy/silver nanocomposites, functionalized silver nanoparticles have been used to detect ammonia, showing high sensing performance with an increase in conductivity[30]. Ppy/NiO nanocomposites used as an anode in lithium-ion batteries have shown improved electrochemical properties compared to pure NiO[31, 32]. Among the functional fillers, transition metal oxides (TMOs) are of particular interest for their potential

*Corresponding author: E-mail: dimplebalan07@gmail.com

use in materials science. Semiconducting transition metal oxides such as ZnO, CuO, NiO, SnO_2, TiO_2, Fe_2O_3, Co_3O_4, and Sb_2O_3 are of particular interest for the detection of pollutants due to their lower cost, non-toxicity, and availability[33-43]. The use of conducting polymers with transition metal oxide nanoparticles is of particular interest in modern science and technology, as they can display the best properties of both materials. Research is still focused on developing new methods for the use of transition metal oxides with conducting polymers, as their interaction can display synergistic effects[44-50]. Zinc oxide (ZnO) is an important semiconductor material with a direct bandgap of 3.4 eV, which possesses a hexagonal crystal structure called wurtzite. It possesses excellent thermal stability, radiation resistance, and various nanostructures, which make it useful in solar cells, gas sensors, biosensors, photo-detectors, surface acoustic wave devices, UV nano-lasers, nano-generators, etc[51]. Though there is limited literature on the electrical characterization of ZnO/Ppy, ZnO is advantageous due to its biocompatibility and lower cost compared to other metal oxides. Despite the difficulty in blending metal oxides with Ppy, encapsulation of metal oxides in the Ppy matrix can improve their physical properties, thus increasing their potential for use in various applications. Accordingly, Ppy-ZnO composite materials were prepared, followed by structural and dielectric property characterization Ppy ($[(C_4H_4–NH)]_n$) is particularly attractive due to its high thermal stability, strong environmental durability, straightforward synthesis, and dopant-dependent conductivity[52]. Its mode of conduction is p-type, which involves bi-polaron transport, hopping of electrons among inter-chain carbon bonds, and dopant-driven movement of ions or cations in the matrix. The conductivity of Ppy is in the range of 10^2 to 7.5×10^3 S-cm^{-1}. It is also possible to control it by altering dopants or other parameters, including conjugation length, polaron formation, and charge transfer efficiency. Composites of conducting polymers are synthesized by incorporating fillers in conducting polymers[53]. The materials have superior properties, unique features, and design opportunities. The properties of conducting polymer composites depend on filler aspect ratio, quality of filler dispersion, orientation, and filler-matrix interactions[54]. The dopants, especially semiconducting metal oxide dopants, have been reported to influence the structural properties of conducting polymers[55-56]. Recent studies have shown that Ppy-based composites, when integrated with ternary oxides, can display highly tunable and enhanced electrical properties. For instance, the successful synthesis of Ppy-coated α-$LiFeO_2$ nanocomposites via the chemical oxidative polymerization method was reported[57]. The Ppy-coated α-$LiFeO_2$ nanocomposites were found to show marked improvements in reversible capacity and cycling stability when tested as the cathode material in lithium-ion batteries. Similarly, the successful fabrication of Ppy/Zn_2SnO_4 nanostructured thin films via the layer-by-layer assembly of Ppy nanospheres and Zn_2SnO_4 hollow spheres reported earlier[58]. The Ppy/Zn_2SnO_4 nanostructured thin films were found to display superior sensitivity in ammonia gas sensing. In another instance, the successful synthesis of doped Ppy/Ag-Ni was reported with sensing applications[59].

Despite the prominent advantages of conducting polymers and transition metal oxides (TMOs), two critical challenges persist in the fabrication of hybrid nanocomposites: (i) the inherent difficulty in achieving uniform, non-aggregated dispersion of inorganic nanoparticles within an organic polymer matrix, and (ii) the subsequent loss of effective surface area and charge transport efficiency due to structural disorder. Traditional synthesis methods often lead to bulk agglomeration, which severely limits the interface-driven quantum effects and hinders the material's electrical conductivity.

Review of the current literature reveals a clear research gap: while spherical or amorphous Ppy/ZnO mixtures are widely reported, studies focused on tailoring a precisely controlled, one-dimensional (1D) cylindrical nanotubular/nanorod morphology with high temperature-dependent electrical stability remain scarce.

To address these challenges, the proposed work introduces a facile, low-temperature chemical oxidative polymerization strategy utilizing methyl orange as a soft-template surfactant. The novelty of this approach lies in using the surfactant to successfully restrict agglomeration, thereby guiding the growth of semi-crystalline, uniform cylindrical nanorods. This specific 1D geometry creates an uninterrupted pathway for electron hopping and bipolaron transport. Consequently, the incorporation of just 5 wt % ZnO leads to a significant enhancement in electrical conductivity paving the way for high-performance applications in supercapacitors and advanced sensing technologies[1].

2. Materials and methods

2.1 Materials

Pyrrole monomer was purchased from Alfa Aesar, whereas ferric chloride ($FeCl_3$) and methyl orange surfactant were supplied by Qualigens. Deionized water with a conductivity of 1 S/m and zinc oxide (ZnO) powder of 99.5 % purity were supplied by High Media. All the chemicals were of analytical grade and high purity.

2.2 Formation of Pure Polypyrrole

For the synthesis of polypyrrole, the monomer pyrrole was polymerized in the presence of methyl orange, which was used as a surfactant. A solution was first prepared by dissolving 5 mM of methyl orange and 1.5 m-mol of ferric chloride ($FeCl_3$) in 30 mL of distilled water with constant stirring. After 30 minutes, 1.5 mM of pyrrole monomer was slowly added to the solution. The solution was left undisturbed at room temperature for 24 hours. After polymerization, washing of the synthesized polymer was carried out three times using water and methanol. The synthesized polymer was then dried in vacuum conditions at 95 °C for 20 hours. Finally, it was grounded into fine powder form for ease of handling.

2.3 Synthesis of Ppy/ZnO Nanocomposites

The Ppy/ZnO nanocomposites containing 5 wt % of zinc oxide were synthesized via an in-situ chemical oxidative polymerization approach to ensure uniform distribution.

The precursor solution containing 5 mM methyl orange surfactant and 1.5 mmol of ferric chloride ($FeCl_3$) oxidant was prepared in 15 mL of distilled water under magnetic stirring. The pre-sonicated ZnO dispersion was then slowly introduced into this surfactant-oxidant mixture under vigorous stirring for 30 minutes to allow the surfactant molecules to coat the ZnO surface. Subsequently, 1.5 mM of pyrrole monomer was added dropwise into the reaction mixture at room temperature. The polymerization was allowed to proceed undisturbed for 24 hours. The resulting black precipitate of Ppy/ZnO nanocomposite was collected, washed repeatedly via centrifugation with water and methanol, and dried in a vacuum oven at 90 °C for 20 hours before being ground into a fine powder[3]. Figure 1 shows the pictorial representation of the entire synthesis process.

2.4 Formation of Pellet

A pellet, 0.8 mm thick and 13 mm in diameter, was fabricated from Ppy and Ppy/ZnO nanocomposites

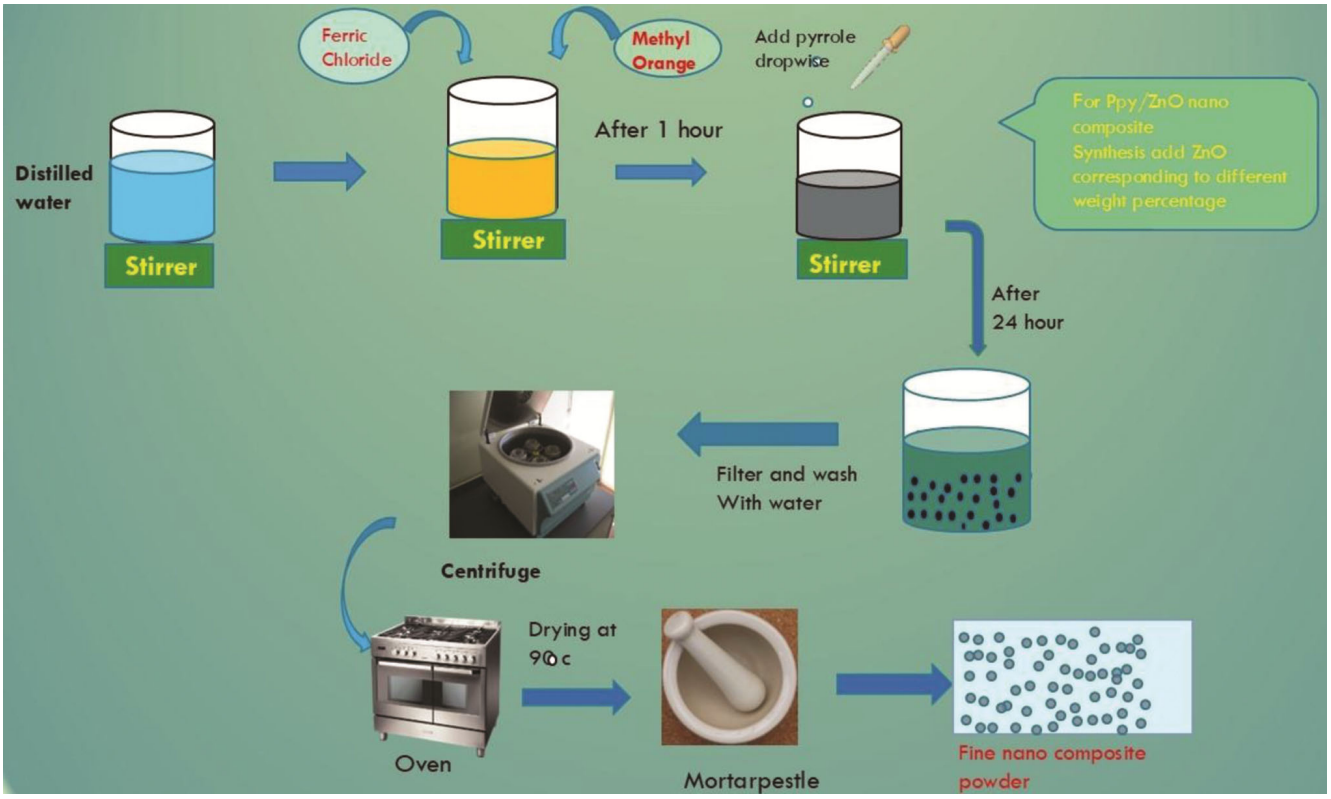

Fig. 1 — Pictorial representation of the entire synthesis process

under a pressure of 80 kg/cm^2. Two silver electrodes were deposited on the pellet's surface, spaced 1 mm apart.

3 Characterization

For XRD analysis, Rigaku Miniflex II X-Ray Diffractometer was used. The XRD technique usesCuK_α radiation with a wavelength of 1.54 Å and nickel as a filter for precise results. The surface characteristics of the fabricated nanocomposites were also studied by FESEM. For FESEM, JEOL 7610F equipment was used. For studying the sensitivity of the fabricated samples in different environmental conditions, measurements were carried out with Keithley 6517B equipment and a DNM-121 nano-ammeter. The changes in the current were continuously recorded by exposing the samples to air, acetone vapor, and then again to air.

4 Results and Discussion

4.1 Structural Investigation

Figure 2 (a–b) presents the X-ray diffraction (XRD) patterns of both pure polypyrrole (Ppy) and Ppy/ZnO nanocomposites. The XRD pattern of pure Ppy displays a broad peak at 2θ = 25.58°, indicating its amorphous nature[60]. In contrast, the Ppy/ZnO nanocomposites exhibit multiple sharp diffraction peaks at 2θ values of 31.84°, 34.56°, 36.32°, 47.62°, 56.76°, 62.96°, 66.53°, 68.10°, 69.24°, 72.68°, and 77.08°, corresponding to the (100), (002), (101), (102), (110), (113), (200), (212), (201), (204), and (202) crystal planes, respectively. These peaks confirm the presence of ZnO with a hexagonal wurtzite crystal structure, matching the standard data from JCPDS card no[61] 79-2205. The crystallite size of ZnO nanoparticles, determined using the Debye Scherrer equation[62-63], was calculated to be approximately 23.56 nm.

$$D = \frac{K\lambda}{\beta cos\Theta}$$

Here, n = 1 indicates first-order diffraction, whereas λ = 1.5406 Å represents the wavelength of the X-ray source. β is the full width at half maximum (FWHM) of the diffraction peak, whereas θ represents the Bragg angle. K is the Scherrer constant. The XRD spectrum of pure polypyrrole shows a broad peak, which indicates that it is amorphous in nature. However, in the case of Ppy/ZnO nanocomposites, sharp peaks have been obtained, which indicates that crystalline features have been developed. This indicates that there is a change in the structure of the materials, from totally amorphous in pure polypyrrole to semi-crystalline in Ppy/ZnOnano-composites[64].

4.2 Field Emission Scanning Electron Microscopy (FESEM)

To understand the surface morphology of nanocomposite materials, a FESEM investigation was performed. Figure 3 (a) shows the pure polypyrrole's FESEM picture. Ppy was observed to consist of cylindrical nanorods with a wide range of sizes. The FESEM micrograph of the polypyrrole/ZnO (5 wt %) nanocomposite is presented in Fig. 3 (b). According to SEM pictures, the Ppy/ZnO nanocomposites also exhibit cylindrical nanorods with cluster morphologies similar to those of polypyrrole. In addition, many small

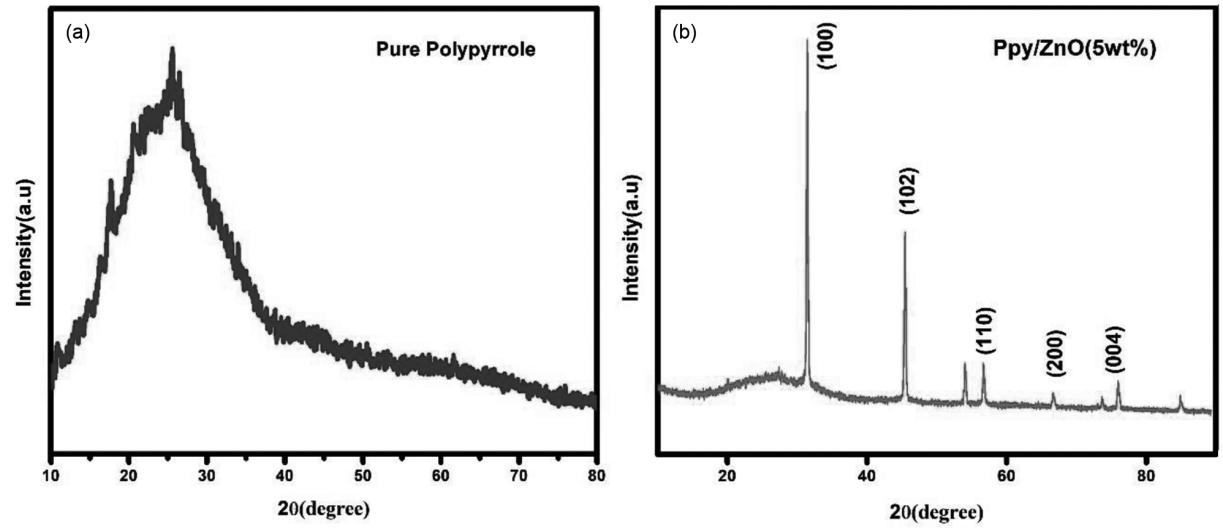

Fig. 2 — XRD patterns of (a) Pure Polypyrrole; and (b) Ppy/ZnO (5wt %) nanocomposites

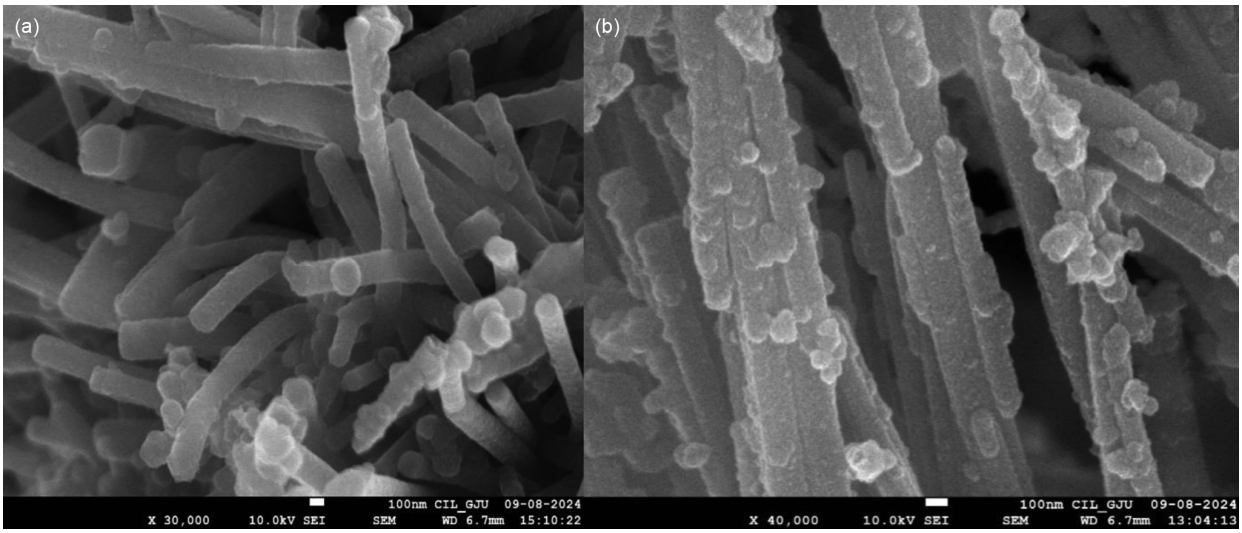

Fig. 3 — SEM image of (a) Pure Polypyrrole; and (b) Polypyrrole /ZnO (5wt %) nanocomposites

particles that may be ZnO particles are scattered around the surface of the layer. The weak interaction between the oxide sample and the polymer chain could be the cause of this.

Zinc oxide is uniformly included on the polypyrrole nanorod in the chemically produced nanohybrid composite material. Since the nanocomposites, as shown in Fig. 3 (b), resemble pure polypyrrole perfectly, a trace quantity of ZnO has no discernible effect on the morphology of polypyrrole. ImageJ software analysis revealed that the nanorods in both Ppy and Ppy/ZnO composites have an average diameter of approximately 135 nm. In polymer-inorganic nanohybrids, loading a higher weight percentage of transition metal oxides often leads to severe particle aggregation due to high surface energy. This agglomeration tends to cover the active polymer sites and completely disrupts the controlled 1D cylindrical structure, turning it into irregular bulk clusters. Such morphological degradation increases charge carrier scattering and drops the overall performance. Therefore, the 5 wt % concentration represents an optimized critical threshold. It is low enough to perfectly preserve the pristine cylindrical nanorod template of Polypyrrole (135nm diameter), yet sufficient to embed fine ZnO nanoparticles on the surface to activate synergistic charge transport and significantly enhance the electrical properties without structural collapse[4].

5 Electrical Conductivity

The DC electrical conductivity of all synthesized samples was investigated across a range of temperatures. The conductivity was calculated using the following standard equation:

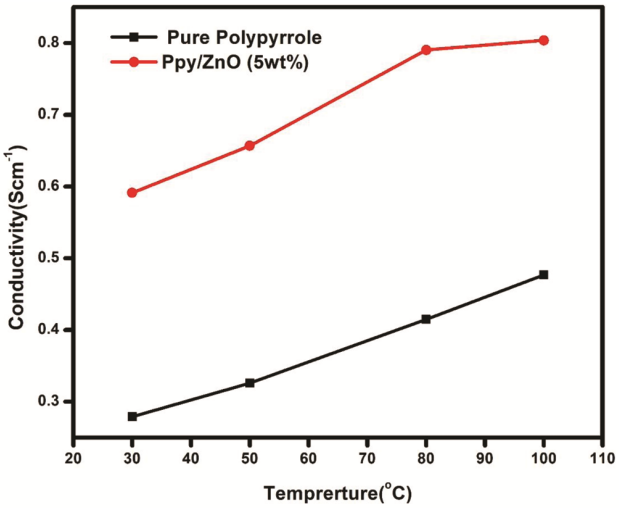

Fig. 4 — Electrical Conductivity ofPure Polypyrrole and Ppy/ZnO (5wt %) at different temperatures

$$\sigma = [\ln 2\ (2S/W)]/[2\pi S\ (V/I)]$$

In this equation, V denotes the applied voltage (V), S represents the spacing between the probes (cm), W is the thickness of the pellet (cm), I is the measured current (A), and σ corresponds to the DC electrical conductivity ($S \cdot cm^{-1}$), respectively[65].

The electrical conductivity of Ppy and Ppy/ZnO nanocomposites at temperatures 40°C,50°C, 60°C, 70°C,80°C,90°C, and 100°C is observed. The electrical conductivity measurements of Ppy and Ppy/ZnO nanocomposites revealed values of 0.279 $S \cdot cm^{-1}$ and 0.5912 $S \cdot cm^{-1}$ at 30 °C, respectively. Upon increasing the temperature to 100 °C, the conductivities increased to 0.476 $S \cdot cm^{-1}$ for Ppy and 0.80385 $S \cdot cm^{-1}$ for Ppy/ZnO, as illustrated in Fig. 4. The incorporation of

ZnO nanoparticles into the polypyrrole matrix led to a notable enhancement in electrical conductivity, which exhibited a further increase with temperature, indicating improved charge transport characteristics relative to pristine Ppy. The mechanism of conductivity in Polypyrrole (Ppy)/ZnO nanocomposites is a complex process that involves the delocalization of electrons along the Ppy chain, as well as the transfer of electrons between Ppy and ZnO nanoparticles. The intrinsic conductivity of Ppy is due to the delocalization of electrons along the polymer chain, which facilitates charge transport through a hopping mechanism. The addition of ZnO nanoparticles enhances the conductivity of the nanocomposite by acting as electron acceptors, facilitating the transfer of electrons from Ppy to ZnO, and increasing the mobility of charge carriers within the Ppy matrix.

The interfacing of p-type Polypyrrole with n-type ZnO nanoparticles creates nanoscale p-nheterojunctions. This configuration facilitates local electron transfer from the HOMO of Ppy to the conduction band of ZnO, acting as an electron-accepting mechanism that effectively elevates the mobile polaron/bipolaron density (n) Electrical conductivity (σ) is dictated by the relation.

$$\sigma = \mu.n.e$$

where n is the charge carrier density, e is the elementary charge, and μ is the carrier mobility

This significant elevation in the mobile polaron/bipolaron density (n) directly increases the volume of active charge carriers available for transport, thereby substantially boosting the overall electrical conductivity (σ) of the nanocomposite[5].

The observed positive temperature coefficient of conductivity increases from 0.5912 $S.cm^{-1}$ at 30°C to 0.80385Scm^{-1} at 100°C for the Ppy/ZnO composite explicitly signifies a thermally activated hopping transport mechanism rather than conventional intrinsic band-gap semiconducting behavior[66]. In conducting polymer matrices, the polymer backbone possesses an amorphous and disordered structural nature, as confirmed by our XRD results. Consequently, the charge carriers (polarons and bipolarons) are heavily localized. As the temperature rises, external thermal energy facilitates the lattice vibrations, lowering the potential barrier width between adjacent conjugated chains. This enables the localized carriers to absorb phonon energy and undergo a inter-chain and intra-chain transport process governed by Mott's Variable-Range Hopping (VRH) model[67-68]. The uniformly embedded crystalline ZnO nanoparticles act as conducting bridges within the cylindrical channels, which significantly reduces the characteristic hopping activation energy. This synergy accelerates the hopping frequency of electrons, leading to the pronounced temperature-dependent enhancement in electrical conductivity[6].

6 Conclusion

The chemical oxidation polymerization process was used to create nanostructured Polypyrrole and Polypyrrole/ZnO with 5 weight percent ZnO concentrations. The structural properties were studied using the X-ray diffraction method. FESEM is used to study the morphology of the prepared materials. When ZnO is 5 weight percent, the Ppy and Ppy/ZnO material's electrical conductivity is measured at temperatures of 40, 50, 60, 70, 80, 90, and 100°C. To conclude, Ppy/ZnO nanocomposite was synthesized using the chemical oxidation method, which is an effective low-temperature method for enhancing the electrical conductivity of materials. Apart from using Ppy/ZnO in other ways, it is also used in supercapacitors due to its antibacterial properties.

In contrast, the significance of our work lies in the successful synthesis of a well-defined 1D cylindrical nanorod/nanotubular morphology achieved via a controlled methyl orange soft-template method. The 1D cylindrical architecture minimizes the grain boundary barriers, allowing a direct pathway for polaron and bipolaron hopping. Unlike typical composites that require high weight percentages of metal oxides to show appreciable electrical changes, our system achieves a profound leap in conductivity 0.279 $S \cdot cm^{-1}$ to 0.5912 $S \cdot cm^{-1}$ at a mere 5 wt% ZnOconcentration. Furthermore, the highly sensitive temperature-dependent linear increment up to 100°C proves that our nanocomposite possesses superior thermal-electrical stability compared to standard amorphous Ppy films, making it a highly significant candidate for next-generation supercapacitors and smart sensing devices[2].

References

1 Chen I P, Chou Y C & Wang P Y, *J Phys Chem C*, 123 (2019) 17864.
2 Bora C & Dolui S K, *Polymer*, 53 (2012) 923.
3 Dhibar S & Das C K, *Ind Eng Chem Res*, 53 (2014) 3495.
4 Qi X, She G, Liu Y, Mu L & Shi W, *Chem Comm*, 48 (2012) 242.
5 Xu K, Li N, Zeng D, Tian S, Zhang S, Hu D & Xie C, *ACS Appl Mater Interfaces*, 7 (2015) 11359.
6 Han Y, Hu N, Liu S, Hou Z, Liu J, Hua X, Yang Z, Wei L, Wang L & Wei H, *Nanotechnol*, 28 (2017) 33LT01.
7 Rawal I, Kumar L, Tripathi R K & Panwar O S, *ACS Omega*, 2 (2017) 7515.

8 Shu K, Wang C, Zhao C, Ge Y & Wallace G G, *Electrochim Acta*, 212 (2016) 561.
9 Zang J, Bao S J, Li C M, Bian H, Cui X, Bao Q, Sun C Q, GuoJ & Lian K, *J Phys Chem C*, 112 (2008) 14843.
10 Janotti A & Van de Walle C G, *Rep Prog Phys*, 72 (2009) 126501.
11 Das T K & Prusty S, *Polym Technol Eng*, 51 (2012) (1487).
12 Guan M, Zhao X, Duan L, Cao M, Guo W, Liu J & Zhang W, *J Appl Phys*, 114 (2013) 114302.
13 Jia Y, Xiaoa P, Heb H, Yaob J, Liub F, Wang Z & Li Y, *Appl Sur Sci*, 258 (2012) 6627.
14 Wang C, Wang Z & Li M, *Chem Phys Lett*, 341 (2001) 431.
15 Fursey G N, *Field Emission in Vacuum Microelectronics* (Kluwer Academic/Plenum Publishers, New York) 2005, p. 99.
16 Ratcliffe N M, *Analytica Chimica Acta*, 239 (1990) 257.
17 Wang F, Gu H & Swager T M, *J Am Chem Soc*, 130 (2008) 5392.
18 Sutar D S, Padma N, Aswal D K, Deshpande S K, Gupta S K & Yakhmi J V, *Sens Actuators B: Chem*, 128 (2007) 286.
19 Jang J & Oh J H, *Chem Commun*, 40 (2004) 882.
20 Ruangchuay L, Sirivat A & Schwank J W, *React Function Polymer*, 61 (2004) 11.
21 Ruangchuay L, Sirivat A & Schwank J, *Talanta*, 60 (2003) 25.
22 Guernion N, Ewen R J, Pihlainen K, Ratcliffe N M & Teare G C, *Synth Metal*, 126 (2002) 301.
23 Barisci J N, Wallace G G, Andrews M K, Partridge A C & Harris P D, *Sens Actuators B: Chem*, 84 (2002) 252.
24 Jang J & Bae J, *Sens Actuators B: Chem*, 122 (2007) 7.
25 Molina J, Fernández J, del Río A I, Bonastre J & Cases F, *Appl Surface Sci*, 257 (2011) 10056.
26 Jia Y, Xiao P, He H, Yao J, Liu F, Wang Z & Li Y, *Appl Surface Sci*, 258 (2012) 6627.
27 Lähdesmäki I, Lewenstam A & Ivaska A, *Talanta*, 43 (1996) 125.
28 Geng L N, Wang S R, Li P, Zhao Y Q, Zhang S M & Wu S H, *Chin J Inorg Chem*, 21 (2005) 977.
29 Virji S, Kaner R B & Weiller B H, *J Phys Chem B*, 110 (2006) 22266.
30 Karmakar N S, Kothari D C & Bhat N V, in *Proceedings of the 57th DAE Solid State Physics Symposium*, 1512 (2013) 294.
31 Idris N H, Wang J-Z, Chou S, Zhong C, Rahman M M & Kun Liu H, *J Mater Res*, 26 (7) (2011) 860.
32 Imani A, Farz G & Ltaief A, *J Nanopart Res*, 11 (2017) 1441.
33 Rahman M M, Ahmed J, Asiri A M & Alamry K A, *New J Chem*, 44 (30) (2020) 13018.
34 Abu-Zied B M, Alam M M, Asiri A M, Ahmed J & Rahman M M, *Microchem J*, 157 (2020) 104972.
35 Subhan M A, Chandra Saha P, Ahmed J, Asiri A M, Al-Mamun M & Rahman M M, *Mater Adv*, 1 (8) (2020) 2831.
36 Subhan M A, Jhuma S S, Saha P C, Ahmed J, Asiri A M, Rifat T P, Raihan T, Azad A K & Rahman M M, *J Environ Chem Eng*, 8 (2020) 104051.
37 Rahman M M, Ahmed J & Asiri A M, *New J Chem*, 43 (48) (2019) 19298.
38 Rahman M M, Ahmed J & Asiri A M, *Biosens Bioelectron*, 99 (2018) 586.
39 Rahman M M & Ahmed J, *Biosens Bioelectron*, 102 (2018) 631.
40 Subhan M A, Chandra Saha P, Sumon S A, Ahmed J, Asiri A M, Rahman M M & Al-Mamun M, *RSC Adv*, 8 (58) (2018) 33048.
41 Subhan M A, Chandra Saha P, Rahman M M, Ahmed J, Asiri A M & AlMamun M, *New J Chem*, 42 (2) (2018) 872.
42 Ahmed J, Rahman M M, Siddiquey I A, Asiri A M & Hasnat M A, *Electrochim Acta*, 246 (2017) 597.
43 Rahman M M, Ahmed J & Asiri A M, *Sens Actuators*, *B Chem*, 242 (2017) 167.
44 Ozkazanc E, Zor S, Ozkazanc H & Gumus S, *Polym Eng Sci*, 53 (2013) 1131.
45 Chang C H, Son P S, Yang J & Choi S, *J Korean Chem Soc*, 53, 2,111 (2009).
46 Jiang L, Jun H-K, Hoh Y-S, Lim C-J, Lee D-S & Huh J-S, *Sens Actuators B*: *Chem*, 105 (2005) 132.
47 Ferreira C A, Domenech S C & Lacaze P C, *J Appl Electrochem*, 31 (2001) 49.
48 Li M, Zhang Y, Yang L, Liu Y & Ma J, *J Mater Sci: Mater Electron*, 25 (6) (2014) 2425.
49 Almond D P, Bowen C R & Rees D A S, *J Phys D: Appl Phys*, 39 (2006) 1295.
50 Eisazadeh H, *World J Chem*, 2 (2) (2007) 67.
51 Dalas E, Mougoyanni P & Sakkopoulas S, *Rom Journ Phys*, 58 (3) (2013) 354.
52 Wang L, Li X & Yang Y, *React Funct Polym*, 47 (2001) 125.
53 Balint R, Cassidy N J & Cartmell S H, *Acta Biomater*, 10 (2014) 2341.
54 Sapalidis A A, Katsaros F K & Kanellopoulos N K, in *Nanocomposites and Polymers with Analytical Methods*, ed. Cuppoletti J (IntechOpen, Croatia) 2011.
55 Aashis S R, Koppalkar R A & Ambika Prasad M V N, *J Appl Polym Sci*, 123 (2012) 1928.
56 Mishra K G & Gupta S C J, *Adv Appl Sci Res*, 2 (2011) 212.
57 Zhang Z J, Zhao W J, Chou S L, Liu H K, Ozawa K & Li H, *Electrochim Acta*, 108 (2013) 820.
58 Zhang D, Wu Z, Zong X & Zhang Y, *Sensor Actuator B Chem*, 274 (2018) 575.
59 Ramesan M T, Santhi V, Bahuleyan B K, Al-Maghrabi M A & Sutar R A, *Mater Chem Phys*, 211 (2018) 343.
60 Upadhyay J & Kumar A, *Compos Sci Technol*, 97 (2014) 55.
61 Kashinath L, Namratha K & Byrappa K, *Appl Surf Sci*, 357 (2015) 1849.
62 Makkar M, Barala M, Nanda K, Gummagoal N & Mohan D, *Physica Scripta*, 100 (6) (2025) 1.
63 Makkar M, Nanda K, Barala M, Kumar C, Gummagoal N & Mohan D, *J Mater Sci: Mater Electr*, 37 (3) (2026) 222.
64 Aaditya V B, Bharathesh B M, Harshitha R, Chaluvaraju B V, Raghavendra U P & Murugendrappa M V, *J Mater Sci: Mater Electr*, 29 (2018) 2848.
65 Husain A, Al-Zahrani S A, Al Otaibi A, Khan I, Mujahid Ali Khan M, Alosaimi A M & Jawaid M, *Polymers*, 13 (11) (2021)1829.
66 Mott N F & Davis E A, *Electronic Processes in Non-Crystalline Materials*, Oxford, 2012.
67 Kaiser A B, *Rep Progress Phys*, 64 (1) (2001) 1.
68 Long Y, Yin Z, Wang M, Zhang Z & Luan J, *Solid State Commun*, 139 (11) (2006) 550.